Journal of Orthopaedic Translation 39 (2023) 43–54

Contents lists available at ScienceDirect

Journal of Orthopaedic Translation

journal homepage: www.journals.elsevier.com/journal-of-orthopaedic-translation

Original article

A static magnetic field enhances the repair of osteoarthritic cartilage by promoting the migration of stem cells and chondrogenesis

Yuting Sun [a,1], Yanwen Fang [b,1], Xinle Li [a,c], Jie Li [a,c], Daquan Liu [a,c], Min Wei [b], Zhongcai Liao [b], Yao Meng [a], Lidong Zhai [a], Hiroki Yokota [d], Lei Yang [e], Ying Yu [f], Ping Zhang [a,c,g,*]

[a] Department of Anatomy and Histology, School of Basic Medical Sciences, Tianjin Medical University, Tianjin, China
[b] Heye Health Technology Co., Ltd., Huzhou, China
[c] Key Laboratory of Hormones and Development (Ministry of Health), Tianjin Key Laboratory of Metabolic Diseases, Tianjin Medical University, Tianjin, China
[d] Department of Biomedical Engineering, Indiana University-Purdue University Indianapolis, IN, USA
[e] Center for Health Sciences and Engineering, Hebei Key Laboratory of Biomaterials and Smart Theranostics, School of Health Sciences and Biomedical Engineering, Hebei University of Technology, Tianjin, China
[f] Department of Pharmacology, Tianjin Key Laboratory of Inflammatory Biology, The Province and Ministry Co-sponsored Collaborative Innovation Center for Medical Epigenetics, School of Basic Medical Sciences, Tianjin Medical University, Tianjin, China
[g] Tianjin Key Laboratory of Spine and Spinal Cord, Tianjin Medical University, Tianjin, China

ARTICLE INFO

Keywords:
Osteoarthritis
Static magnetic field
Mesenchymal stem cells
Chondrogenesis
SDF-1/CXCR4
Piezo1

ABSTRACT

Objective: To investigate the therapeutic effects of static magnetic field (SMF) and its regulatory mechanism in the repair of osteoarthritic cartilage.
Methods: Fourteen-week-old female C57BL/6 mice were randomly divided into the sham operation group and the osteoarthritis (OA) groups with and without SMF application. SMF was applied at 200 mT for two consecutive weeks. Changes in knee cartilage were examined by histomorphometry, and the chondrogenesis and migration of endogenous stem cells were assessed. The expression of SRY-related protein 9 (SOX9), Collagen type II (COL2), matrix metallopeptidase 13 (MMP13), stromal cell-derived factor 1/C-X-C chemokine receptor type 4 (SDF-1/CXCR4), Piezo1 and other genes was evaluated, and the mechanism of SMF's action was tested using the CXCR4 inhibitor, AMD3100, and Piezo1 siRNA.
Results: SMF significantly decreased the OARSI scores after induction of OA. SMF was beneficial to chondrogenesis by elevating SOX9. In the OA mouse model, an increase in MMP13 with a decrease in COL2 led to the destruction of the cartilage extracellular matrix, which was suppressed by SMF. SMF promoted the migration of cartilage-derived stem/progenitor cells and bone marrow-derived mesenchymal stem cells (MSCs). It increased SDF-1 and CXCR4, while the CXCR4 inhibitor significantly suppressed the beneficial effects of SMF. The application of Piezo1 siRNA inhibited the SMF-induced increase of CXCR4.
Conclusion: SMF enhanced chondrogenesis and improved cartilage extracellular matrices. It activated the Piezo1-mediated SDF-1/CXCR4 regulatory axis and promoted the migration of endogenous stem cells. Collectively, it attenuated the pathological progression of cartilage destruction in OA mice.
The Translational potential of this article: The findings in this study provided convincing evidence that SMF could enhance cartilage repair and improve OA symptoms, suggesting that SMF could have clinical value in the treatment of OA.

Abbreviations: BMSCs, Bone marrow mesenchymal stem cells; CC, Calcified cartilage; CD105, Endothelial glycoprotein; CD146, Melanoma cell adhesion molecule; CD166, Activated leukocyte adhesion molecule; COL2, CollagenII; CSPCs, Cartilage-derived stem/progenitor cells; CXCR4, C-X-C chemokine receptor type 4; HC, Hyaline cartilage; MMP13, Matrix metallopeptidase 13; MSCs, Mesenchymal stem cells; mT, Millitesla; OA, Osteoarthritis; OARSI, Osteoarthritis Research Society International; SDF-1, Stromal cell-derived factor 1; SMF, Static magnetic field; SOX9, SRY-related protein 9; TAC, Total articular cartilage.

* Corresponding author. Department of Anatomy and Histology School of Basic Medical Sciences Tianjin Medical University, 22 Qixiangtai Road, Tianjin, 300070, China.
E-mail address: pizhang2008@163.com (P. Zhang).
[1] These authors contributed equally to the study

https://doi.org/10.1016/j.jot.2022.11.007
Received 23 August 2022; Received in revised form 26 November 2022; Accepted 30 November 2022

1. Introduction

Osteoarthritis (OA) is the most common degenerative joint disease and the leading cause of disability, affecting more than 300 million people worldwide [1,2]. The hallmark of OA is the loss of articular cartilage that cushions the joint during exercise [3]. The ability of chondrocytes to repair themselves is limited due to insufficient blood supply and the low number of stem cells in the cartilage [4]. Treatments for knee OA include drug therapy, physical therapy, and surgery, which are aimed at reducing pain and improving basic function. As OA worsens, it is usually resolved with the surgical implantation of artificial joints [1]. However, artificial joints have a limited lifespan and are not suitable for the treatment of early OA [5]. Thus, an effective regimen to attenuate the pathological progress of OA is urgently needed.

A static magnetic field (SMF) is a magnetic stimulation with a constant magnetic intensity in a fixed direction. According to field strengths, SMF can be divided into hypo (<5 μT), weak (5 μT-1 mT), moderate (1 mT-1 T), and high (>1 T) [6]. Recently, SMF at an intensity range of 4–200 mT has been used for the non-invasive treatment of bone diseases such as nonunion, fracture, and osteoporosis [7]. Considering the cost, adverse effects, and potential risks of drugs or surgical operations, non-invasive and handy SMF is potentially considered a physical therapeutic option [8,9]. Preclinical studies have shown that SMF can promote the proliferation, migration, adhesion, and differentiation of mesenchymal stem cells (MSCs) and improve cartilage defects [10,11]. However, the role of MSCs migration and the mechanism of SMF-driven chondrogenesis of osteoarthritic cartilage are yet to be elucidated.

MSCs, with the ability to develop a variety of tissue lineages, have been championed as a promising therapeutic source for the repair and regeneration of degenerative, inflammatory, or autoimmune diseases [12,13]. MSCs can differentiate into chondrocytes after migration to the site of joint injury. SRY-related protein 9 (SOX9) is a major transcription factor involved in a series of subsequent events in chondrogenesis, which is reduced in the articular cartilage of patients with OA [14]. Up-regulation of SOX9 is one of the key upstream chondrogenic events leading to the production of collagen type II (COL2), which is a major extracellular matrix protein [15]. Evidence suggests that matrix metalloproteinase 13 (MMP13) is an important cofactor or disease mediator and it degrades the extracellular matrix [3]. However, it is unclear whether SMF improves articular cartilage by regulating SOX9, MMP13, and COL2.

Based on the co-expression of cell surface markers such as CD166, CD146, and CD105, cartilage-derived stem/progenitor cells (CSPCs) were found in normal and OA human articular cartilage. The ability of these cells to differentiate into adipocytes or osteocytes is reported analogous to that of bone marrow-derived MSCs (BMSCs) [16], which are involved in tissue homeostasis [17]. The percentage of CSPCs in osteoarthritis cartilage was ~8%, while that in normal cartilage was ~4% [16]. By contrast, BMSCs are easy to sample, isolate, and amplify *in vitro* and have become popular seed cells in cartilage tissue engineering [18]. BMSCs migrate from the bone marrow to the damaged tissue when they sense the damage signal, which is regulated by a variety of mechanical and chemical factors [19]. Thus, in the treatment of OA, physical therapy is often used to promote the migration of stem cells [20,21]. It is reported that the stromal cell-derived factor 1 (SDF-1)/C-X-C chemokine receptor type 4 (CXCR4) axis plays a key role in inducing BMSCs to migrate to injury sites and participate in tissue regeneration [19]. Thus, increasing the expression of CXCR4 is a potential strategy to improve the migration of BMSCs and accelerate tissue repair [22]. Our previous study has shown that physical stimulation can promote the migration of MSCs in OA mice by activating SDF-1/CXCR4 signaling [5]. In addition, the Piezo1 channel, as a key mechanical sensor, can convert mechanical stimuli into electrochemical signals *in vivo* [23]. As a physical therapy, a question herein was whether SMF can activate Piezo1 and influence the migration of CSPCs.

We hypothesized that SMF enhances the repair of osteoarthritic cartilage by promoting the migration and chondrogenesis of CSPCs *in vivo*. BMSCs and ST2 cells were used in *in vitro* studies to investigate SMF-driven mechanisms of the regulation of CSPCs. SMF can activate the SDF-1/CXCR4 signal by regulating Piezo1 expression, thereby promoting the migration ability of MSCs. To test this hypothesis, we used a mouse OA model to evaluate the effects of SMF. The Osteoarthritis Research Society International (OARSI) score was used to assess the degree of cartilage destruction. The influence of SMF on CSPCs was observed by co-staining the markers of CSPCs with immunofluorescence. We also examined the expression of SOX9, MMP13, COL2, SDF-1, CXCR4, Piezo1, and other genes by Western blot analysis, immunohistochemistry, and immunofluorescent analyses. To explore the mechanism, AMD3100 (an inhibitor of CXCR4) and Piezo1 siRNA were used in mouse bone marrow-derived stem cells and ST2 mouse bone marrow stromal cells.

2. Materials and methods

2.1. Animals and materials preparation

Female C57BL/6 mice (14 weeks old, Animal Center of Academy of Military Medical Sciences, Beijing, China) were used (approval number SCXK (Jing): 2022–0002). All experiments were approved by the Ethics Committee of Tianjin Medical University and were carried out in accordance with the *Guide for the Care and Use of Laboratory Animals* (National Institutes of Health, Bethesda, MD, USA). Mice were housed under pathogen-free conditions and were fed with mouse chow and water *ad libitum*. Mice were allowed to move freely in plastic cages at room temperature (25 °C) with a 12-h light/dark cycle.

DMEM, fetal bovine serum (FBS), penicillin, streptomycin, and trypsin were purchased from Invitrogen (Carlsbad, CA, USA). TGF-β3 was purchased from Novoprotein (Shanghai, China), and 3,3′-diaminobenzidine (DAB) substrate kit and the immunohistochemical staining kit were obtained from ZSGB-BIO (Beijing, China). Other chemicals were purchased from Millipore Sigma (St. Louis, MO, USA) unless otherwise stated.

2.2. Experimental design and OA surgery

In the first set of experiments, forty-five mice were used to evaluate the effect of SMF in the OA mice. These mice were divided into three groups: the sham operation group (Sham, n = 15), the OA group (OA, n = 15), and the SMF-treated OA group (OAS, n = 15). The mouse in OA and OAS groups received OA surgery on both knees, and the Sham group received a sham operation on both knees. The SMF exposure therapy was administered for consecutive two weeks, and then these mice were sacrificed.

In the second set of experiments, eighteen mice were employed to assess the effect of SMF on OA cells *in vitro*. These mice were divided into the sham operation group and the OA group. The cells extracted from the sham operation group were marked Sham (n = 6). The cells obtained from the OA mice without and with SMF were labeled as OA (n = 6) and OA + SMF (n = 6), respectively.

OA surgery was performed as previously described [24]. Briefly, the surgery was performed using a sterile technique and under anesthetic with 1.5% isoflurane (IsoFlo, Abbott Laboratories, Abbott Park, IL) at a flow rate of 1.0 L/min. Prior to making a 20-mm incision to expose the knee joint, the left hindlimb was shaved and disinfected with 70% alcohol solution. The medial collateral ligament was transected and the articular cavity was opened to allow for the removal of the medial meniscus (Fig. 1A). The surgery site was rinsed with sterile saline, and the incision was closed. The same procedure was conducted on the right knee, and 1% pramoxine hydrochloride ointment was applied to the incision sites for the first 3 postoperative days.

2.3. SMF exposure system

In animal experiments, a permanent magnet (310 × 130 × 35 mm), which consisted of 16 alternately inserted magnets, was placed under the

mouse cage for two consecutive weeks (Fig. 1B&C). In cell culture studies, a set of permanent magnets (35 mm in diameter and 10 mm in thickness) were placed beneath cell plates (Fig. 1D). The intensity of SMF was measured using a Gauss meter. The magnetic field intensity was controlled by adjusting the distance between the magnet and the culture plate. ST2 cells were employed to evaluate the responses to SMF0, SMF50, SMF100, and SMF200, which corresponded to intensities of 0, 50, 100, and 200 mT, respectively. Based on the pre-experimental results, the suitable magnetic field intensity was selected (All $p < 0.05$; Supplementary Fig. 1).

2.4. Histological analysis

After the mice were sacrificed on day 14, the knee joints were dissected, fixed in 10% neutral buffered formalin for two days, and decalcified in 14% ethylene diamine tetra-acetic acid (EDTA, pH 7.4) for two weeks. The decalcified knee joint specimens were embedded in paraffin and cut into 5-μm thick coronal slices. The histopathological grade of the cartilage was assessed on the Safranin O-stained slides using the OARSI scoring system [25]. In addition, the ratio of calcified cartilage to the total articular cartilage (CC/TAC), chondrocyte numbers, and vacuolar cell numbers were measured in a blinded fashion.

2.5. Cell culture

After the mice were sacrificed, the BMSCs were collected by flushing the femur and tibia with DMEM basic containing 2% FBS. Mononuclear cells were isolated by low-density gradient centrifugation with Ficoll (Sigma, USA) [26]. Afterward, they were cultured in MesenCult basal medium with MesenCult supplement to obtain BMSCs. The BMSCs were cultured in DMEM containing 10% FBS, 100 U/mL penicillin, and 0.1 mg/mL streptomycin. ST2 cells were cultured in DMEM supplemented with 10% FBS and 1% penicillin/streptomycin. BMSCs isolated from mice were cultured in osteogenic, chondrogenic, and adipogenic differentiation media. BMSCs have three lineage potentials (osteogenesis, chondrogenesis, and adipogenesis), and we presented the images of differentiated cells in Supplementary Fig. 2.

2.6. SiRNA transfection

Three siRNAs targeting Piezo1 (siRNA1—sense: 5′-GUCUCAAGAACUUCGUAGATT-3′, antisense: 5′-UCUACGAAGUUCUUGAGACTT-3′; siRNA2—sense: 5′-GCUUGCUAGAACUUCACGUTT-3′, antisense: 5′-ACGUGAAGUUCUAGCAAGCTT-3′; siRNA3—sense: 5′-GUCAGUUCGUGAAGGAGAATT-3′, antisense: 5′-UUCUCCUUCACGAACUGACTT-3′) and a scrambled siRNA (sense: 5′-UUCUCCGAACGUGUCACGUTT-3′, antisense: 5′-ACGUGACACGUUCGGAGAATT-3′) were synthesized by GenePharma Biotechnology (Shanghai, China). ST cells were transfected with siRNA using a GP-transfect-Mate (GenePharma Biotechnology, Shanghai, China) following the manufacturer's protocol. The silencing efficiency was determined 48 h post-transfection by Western blot analysis [27]. Piezo1 siRNA was cultured with stromal cells before the application of SMF.

2.7. Chondrogenic assays

BMSCs were cultured in 6-well plates at 2×10^6 cells/well in a chondrogenic differentiation medium containing high-glucose DMEM supplemented with 10 mmol/L β-glycerophosphate, 10^{-8} mol/L dexamethasone, and 50 μg/mL ascorbic acid 2-phosphate, for up to 28 days in the presence of 10 ng/mL of transforming growth factor-β3. We changed the medium every other day, and the cells in the OA + SMF group were exposed to the SMF for the first two weeks. The cells were fixed in 10% buffered formalin for 30 min at room temperature, washed with PBS for

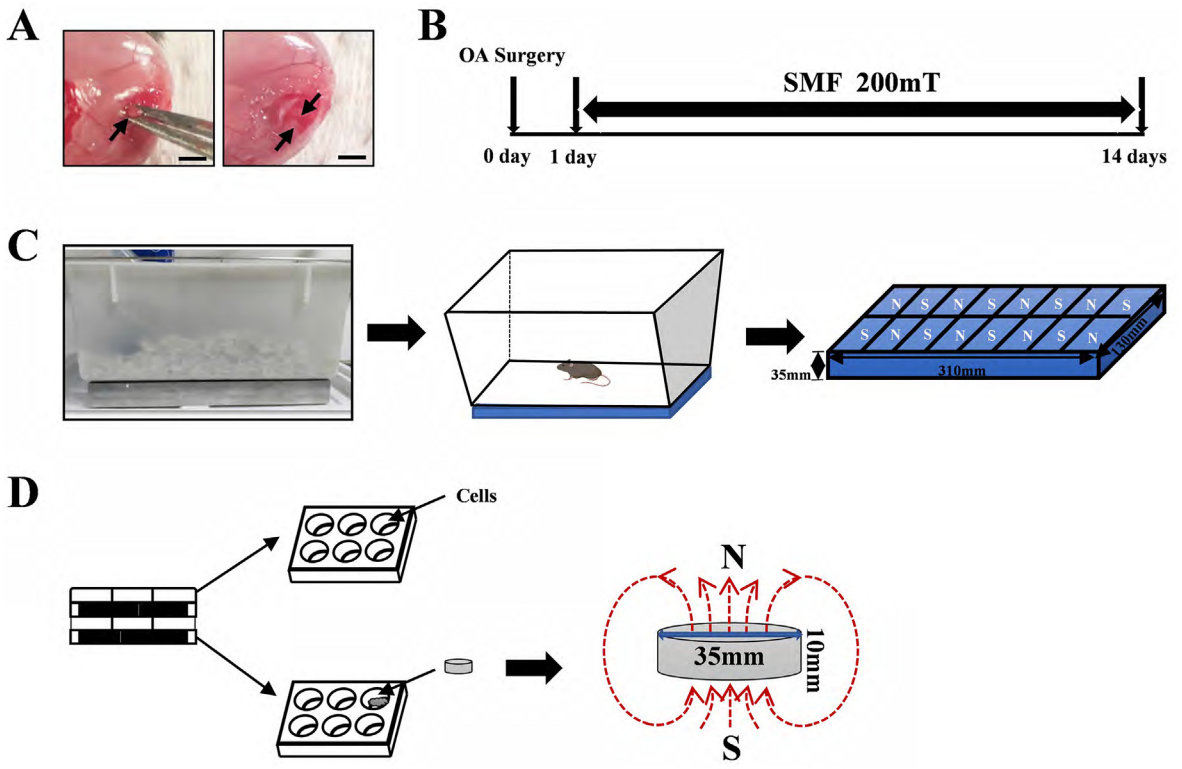

Figure 1. OA surgery, experimental timeline, and setup of the SMF *in vivo* and *in vitro* (A) The medial collateral ligament was transected and the medial meniscus was removed on the left knee to induce osteoarthritis. Arrows indicated medial meniscus ligament (left), and articular surfaces of femur and tibia (right). Bar = 1 mm (B) Experimental timeline (C) Experimental setup of SMF for the mice exposure experiments (D) The permanent magnet assembled beneath the cell plates generates an SMF environment.

one time, and incubated with 1% Alcian blue in 0.1 M HCl (pH 1.0) for at least 2 h. Chondrogenic cells were visualized as blue-stained cells, and their number was counted in a blinded fashion under a microscope (200 × magnification) [3].

2.8. Quantitative RT-PCR

Quantitative RT-PCR (qRT-PCR) was conducted for chondrocytes and ST2 bone marrow stromal cells, which were grown in DMEM with 10% FBS and 1% antibiotics [26]. Transcript levels of SOX9, Piezo1, and CXCR4, as well as β-actin as the reference gene for normalization of expression levels, were determined. The cells in the OA + SMF group were exposed to the static magnetic field for the first two weeks. Total RNA was extracted by a TransZol Up Plus RNA Kit ER501 (Transgen, Beijing, China) and reverse-transcribed into complementary DNA (cDNA) by cDNA Synthesis SuperMix AT341 (Transgen). The diluted cDNA and specific primers were added to 2 × PerfectStart Top Green qRT-PCR SuperMix (Transgen). The specific primers were designed and synthesized by Sangon Biotech (Shanghai, China), and their sequences are listed in Table 1. The expression levels were determined by the $2^{-\Delta\Delta Ct}$ method, and the technical triplicates were used for each experiment.

2.9. Transwell migration assay

The migration of BMSCs was performed using a 24-well transwell chamber (8 μm pore size). BMSCs (2×10^4 cells/well) were suspended in 100 μL of serum-free culture medium with or without AMD3100 (an inhibitor of CXCR4) (10 μg/ml). Cells were placed into the upper chamber, and 500 μL DMEM medium containing 10% FBS was added to the bottom chamber [5]. After incubation at 37 °C and 5% CO_2 for 12 h, the upper surface of the transwell filters was swabbed to remove cells. Cells on the underside of the filter, representing the migrated cells, were fixed in 10% of neutral-buffered formalin and stained with 0.1% crystal violet. The number of migrated cells was counted in a blinded fashion.

2.10. Wound healing assay

BMSCs, extracted from primary bone marrow cells, were seeded in 6-well culture plates and grown to nearly 100% confluence. Scratches were made by a 200-μL pipette tip to form a linear scratch on the monolayer BMSCs [28]. The inhibitor group received AMD3100 (10 μg/ml) after the scratching operation, and the supernatant cells were removed with PBS. Images of each scratch were taken at 0 and 24 h at 100 × magnification, and the ratio of the healed wound area to the total wound area was determined with 3 wells per group in a blinded fashion.

2.11. Immunohistochemical staining

Immunohistochemical staining was performed using an immunohistochemical kit and DAB substrate kit according to the manufacturer's protocol. Knee coronal sections were incubated with primary antibodies against SOX9 (Abcam, Cambridge, MA; dilution 1:1000), MMP13 (Abcam; dilution 1:200), COL2 (Abcam; dilution 1:200), and CXCR4 (Abcam; dilution 1:200) at 4 °C overnight. The ratio of the positively stained cells by the primary antibodies to the total cells was determined in a blinded fashion.

Table 1
Primer sequences used for polymerase chain reactions.

Gene	Sequence
SOX9	Forward primer (5′–3′): AGGTGCTGAAGGGCTACGACTG
	Reverse primer (5′–3′): TCGCTTGACGTGTGGCTTGTTC
Piezo1	Forward primer (5′–3′): CTCCCTGTTACGCTTCAATGCTCTC
	Reverse primer (5′–3′): GTGACCTGGTATGCTGTGTCTTGAG
CXCR4	Forward primer (5′–3′): CCTGCCCACCATCTACTTCATCATC
	Reverse primer (5′–3′): GGTACTTGTCCGTCATGCTCCTTAG
β-actin	Forward primer (5′–3′): ATCTGGCACCACACCTTCTACAATG
	Reverse primer (5′–3′): ATCTGGGTCATCTTTTCACGGTTGG

Abbreviations: CXCR4, C-X-C chemokine receptor type 4; SOX9, SRY-box 9

2.12. Immunofluorescence staining

For immunofluorescence staining, paraffin-embedded knee joint sections were blocked with 5% goat serum for 30 min and stained with primary antibodies against CD166 (ImmunoWay; dilution 1:100), CD146 (ImmunoWay; dilution 1:100), CD105 (ImmunoWay; dilution 1:100), and SDF-1 (Abcam; dilution 1:100) overnight at 4 °C. Sections were then stained with Alexa 488 or Alexa 594 dye-labeled secondary antibodies (Life Technologies, Carlsbad, CA) while avoiding light. Nuclei were labeled with 4, 6-diamidino-2-phenylindole (DAPI), and images were obtained using a U-RFL-T fluorescence microscope (Olympus, Tokyo, Japan). The experimental procedures of double immunofluorescent staining and fluorescence staining were mostly identical. The number of positively stained cells and total cells per specimen were counted in a blinded fashion.

For cellular immunofluorescence, cells cultured on coverslips were fixed with ethanol and then treated with 0.5% Triton X-100 (Sigma Aldrich, Germany) in PBS. Ten % blocking serum was used to block nonspecific binding and stained with primary antibodies against SOX9 (Abcam, Cambridge, MA; dilution 1:1000), MMP13 (Abcam, Cambridge, MA; dilution 1:200), COL2 (Abcam, Cambridge, MA; dilution 1:200), Piezo1 (Proteintech; dilution 1:500), and CXCR4 (Abcam, Cambridge, MA; dilution 1:200) overnight at 4 °C. The tissue immunofluorescence procedure was then followed, and the fluorescence intensity of positively stained cells was determined by Image J.

2.13. Western blot analysis

Cartilage tissues, BMSCs, and ST2 cells were lysed in a RIPA lysis buffer to isolate proteins. Equal amounts of proteins were denatured and resolved by 8% sodium dodecyl sulfate-polyacrylamide gel electrophoresis. Proteins were transferred to polyvinylidene fluoride membranes, incubated with 5% skim milk for 1.5 h at room temperature, and then incubated for 12–16 h at 4 °C with primary antibodies specific to SOX9 (Abcam), MMP13 (Abcam), COL2 (Abcam), CXCR4 (Abcam), Piezo1 (Proteintech). Beta-actin (Cell Signaling Technology) was used as the loading control. The membranes were incubated with horseradish peroxidase (HRP)-conjugated secondary antibody, which was dissolved in a blocking buffer, for 2 h at room temperature. Protein bands were detected using an enhanced chemiluminescent kit (Thermo Fisher Scientific) [29]. The signal intensity of SOX9, MMP13, COL2, CXCR4, and Piezo1 was normalized to β-actin intensity.

2.14. Statistical analysis

Data were analyzed using GraphPad Prism version 25.0 and were expressed as the mean ± S.D. Statistical significance among groups was examined by one-way ANOVA, followed by a post-hoc test using Fisher's protected least significant difference. The student's *t*-test was conducted for two-group comparison. All comparisons were two-tailed and statistical significance was assumed at $p < 0.05$. The asterisks (*, ** and ***) represent $p < 0.05$, 0.01, and 0.001, respectively.

3. Results

3.1. SMF reduced articular cartilage degeneration

Safranin O staining was conducted to evaluate the effect of SMF on articular cartilage. Compared to the sham group, the OARSI score of the articular cartilage in the OA mice was increased ($p < 0.001$; Fig. 2A&B).

However, the OAS group significantly reduced the OARSI scores ($p < 0.01$).

The tidemark is the dividing line between the hyaline and calcified cartilage. Hyaline cartilage (HC) thickness is the distance from the tibial cartilage surface to the tidemark. Calcified cartilage (CC) thickness is the distance from the tidemark to the subchondral bone plate. Total articular cartilage (TAC) thickness is the distance from the surface of the cartilage to the subchondral bone plate. Histopathology of articular cartilage sections showed that in OA mice the calcified cartilage thickness was increased with a decrease in the hyaline cartilage thickness ($p < 0.001$; Fig. 2C). Also, the tidemark moved toward the articular surface. However, the ratio of calcified cartilage to total articular cartilage was reduced in the OAS group ($p < 0.001$). We also evaluated chondrocytes and vacuolar cells in the medial plateau region of the tibia. Compared to the sham group, the chondrocytes in the OA mice were significantly decreased ($p < 0.001$; Fig. 2D). However, they were considerably increased after SMF treatment ($p < 0.001$). By contrast, the number of vacuolar cells was increased in the OA mice ($p < 0.001$; Fig. 2E), while they were decreased in the OAS group ($p < 0.001$).

3.2. SMF improved chondrogenic differentiation and cartilage matrix

To evaluate the effect of SMF on the chondrogenic differentiation of BMSCs, Alcian blue staining was performed after 28 days of chondrogenesis induction (Fig. 2F). The images at a magnification (200 ×) were shown in Supplementary Fig. 3. Compared to the sham group, the number of differentiated chondrocytes in the OA group was significantly reduced ($p < 0.001$; Fig. 2G), but it was restored in the OAS group ($p < 0.001$). The study also determined the expression of SOX9 in the knee cartilage using immunohistochemical staining (Fig. 3A). Compared to the sham group, $SOX9^+$ cells were significantly decreased in the OA mice ($p < 0.001$; Fig. 3B), while they were increased after SMF treatment for two weeks ($p < 0.001$). The mRNA and protein levels of SOX9 were consistent with the immunohistochemical result (all $p < 0.05$; Fig. 3C–E).

To determine the effects of SMF on the extracellular matrix in articular cartilage, we detected the expression of MMP13 and COL2 in knee cartilage by immunohistochemistry staining (Fig. 3F&H). The results showed that the $MMP13^+$ cells in the OA group were remarkably increased ($p < 0.001$; Fig. 3G), while the OAS group decreased them ($p < 0.001$). In contrast, the $COL2^+$ cells in the OA group were decreased

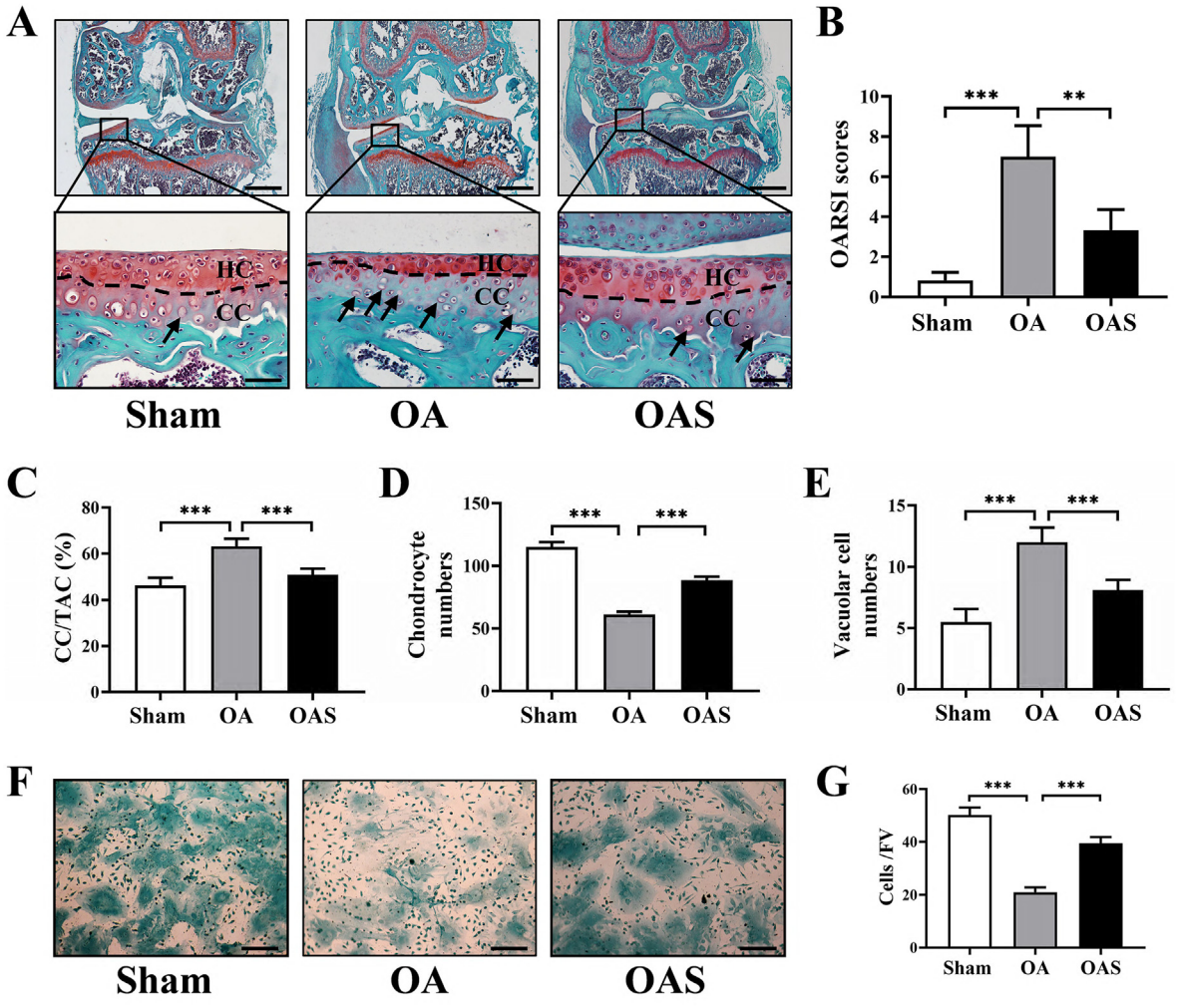

Figure 2. SMF reduced articular cartilage damage and increased the number of chondrocytes (A) Representative Safranin O-stained images. The arrows indicate vacuolar cells, and the black dotted lines represent the tide line. Bar (upper) = 500 μm and bar (lower) = 50 μm (B–E) Quantification of OARSI scores, the value of CC/TAC, chondrocyte numbers, and vacuolar cell numbers in the area proximal to the subchondral bone of the medial tibial plateau; n = 12 (F–G) Representative images of the Alcian blue-stained chondrocytes, induced by mouse-derived BMSCs, and the quantification of the chondrocyte numbers (FV, field of view) *in vivo*. Bar = 50 μm; n = 3. $^{**}p < 0.01$, $^{***}p < 0.001$.

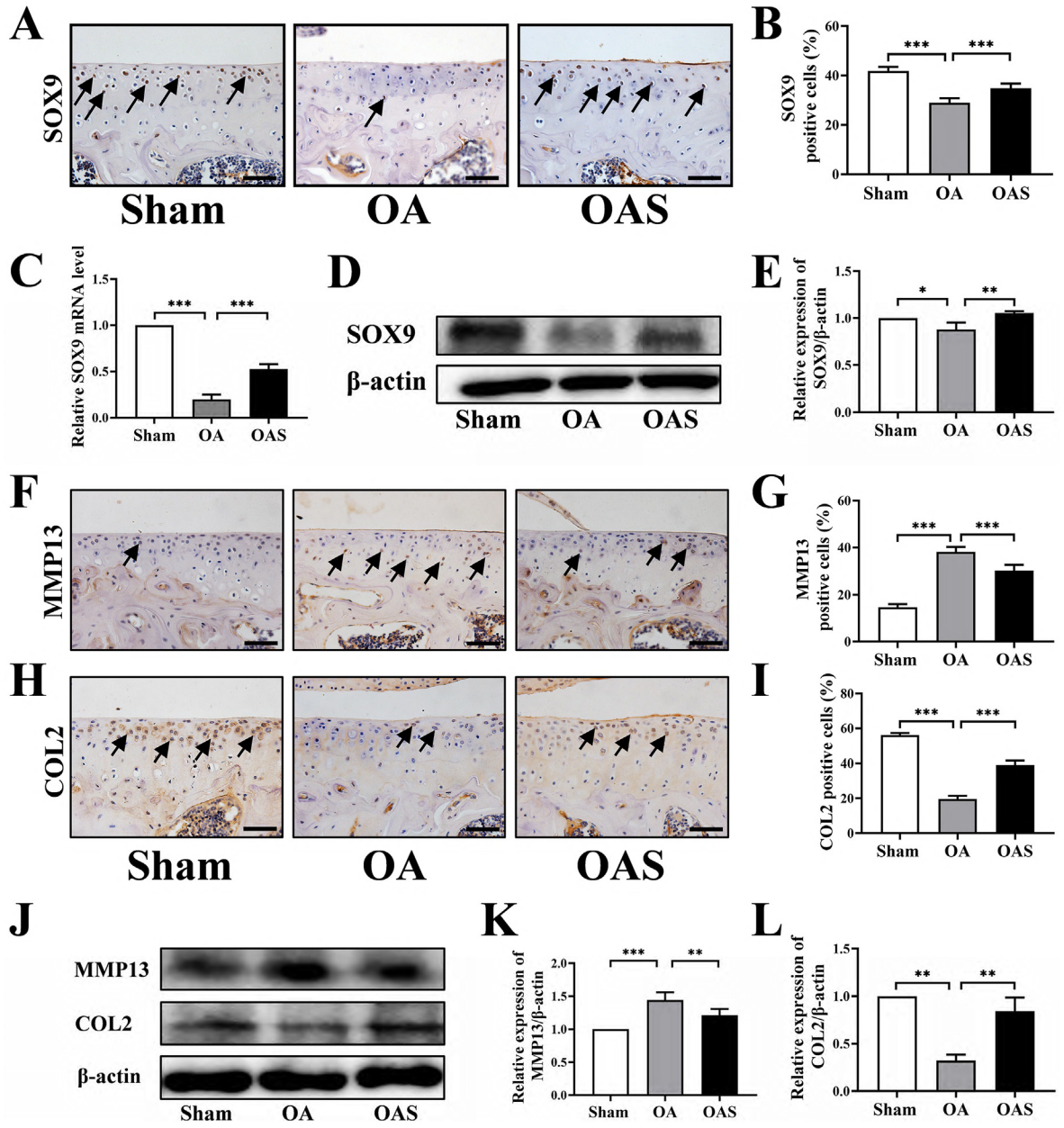

Figure 3. Effect of SMF on the chondrogenesis and cartilage extracellular matrix *in vivo* (A) Representative immunohistochemical images of SOX9 in articular cartilage. Bar = 50 μm (B) Quantification of $SOX9^{+}$ cells in articular cartilage; n = 12 (C) The mRNA expression of SOX9 in articular cartilage was examined by qRT-PCR. n = 3 (D–E) Western blot analysis showing the protein level of SOX9 and the relative quantification of the protein level of SOX9 in articular cartilage; n = 3 (F, H) Representative immunohistochemical images of MMP13 and COL2 in articular cartilage. Bar = 50 μm. (G, I) Quantification of $MMP13^{+}$ and $COL2^{+}$ cells in articular cartilage; n = 12. (J-L) Western blot analysis, showing the protein levels of MMP13 and COL2 and the relative quantification of the protein levels of MMP13 and COL2 in articular cartilage; n = 3. *$p < 0.05$, **$p < 0.01$, ***$p < 0.001$.

compared to the sham group ($p < 0.001$; Fig. 3I), and they were increased in the OAS group ($p < 0.001$). This result was consistent with Western blot analysis (all $p < 0.01$; Fig. 3J-L).

3.3. SMF decreased the MMP13 and increased the COL2, and SOX9 in vitro

The influence of SMF on the chondrogenic differentiation of BMSCs extracted from OA mice was observed after the treatment of BMSCs with SMF (OA + SMF group) for 2 weeks *in vitro*. After 28 days of chondrogenesis induction, Alcian blue staining showed that the number of differentiated chondrocytes in the OA + SMF group was significantly increased after 14 days of SMF exposure ($p < 0.001$; Fig. 4A&B). These images at a magnification (200 ×) were shown in Supplementary Fig. 3. To further validate the effect of SMF on markers of chondrogenesis, SMF was applied to OA mouse-derived BMSCs for two weeks, followed by immunofluorescence staining on day 14 to examine the induction of chondrogenesis (Fig. 4C). The results showed that compared to the sham group, the fluorescence intensity of SOX9 in the OA group was decreased ($p < 0.001$; Fig. 4D), but it was restored by the two-week SMF ($p < 0.01$). The images at a magnification (200 ×) were shown in Supplementary Fig. 4. This result was consistent with qRT-PCR (both $p < 0.01$; Fig. 4E).

To further examine the effect of SMF on the extracellular matrix, we quantified the levels of MMP13 and COL2 using immunofluorescence staining on the 14th day of chondrogenesis induction and SMF exposure (Fig. 4F&H). Compared to the sham group, the fluorescence intensity of

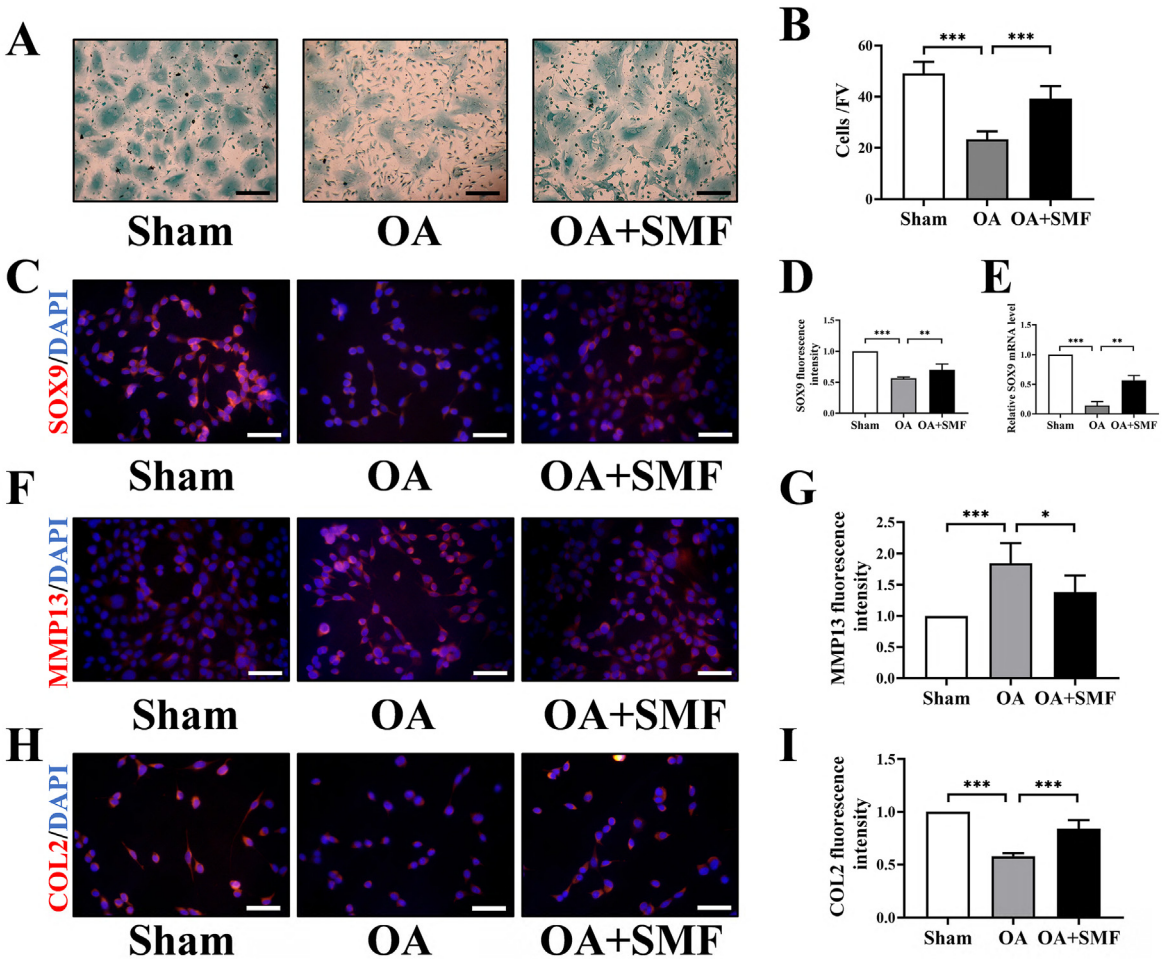

Figure 4. Effects of SMF on BMSCs chondrogenesis and cartilage matrix *in vitro* (A–B) Representative images of murine BMSC-induced chondrocytes stained with Alcian blue and quantification of the chondrocyte numbers (FV, field of view) *in vitro* (C) Representative immunofluorescence images of SOX9 on the 14th day of chondrogenesis induction. Bar = 50 μm (D) Quantification of the fluorescence intensity of SOX9; n = 3 (E) The mRNA expression of SOX9 on day 14 of chondrogenesis induction was examined by qRT-PCR; n = 3 (F) Representative immunofluorescence images of MMP13 on day 14 of chondrogenesis induction. Bar = 50 μm (G) Quantification of the fluorescence intensity of MMP13; n = 3 (H) Representative immunofluorescence images of COL2 on the 14th day after chondrogenesis induction. Bar = 50 μm (I) Quantification of the fluorescence intensity of COL2; n = 3. *$p < 0.05$, **$p < 0.01$, ***$p < 0.001$.

MMP13 in the OA group was increased ($p < 0.001$; Fig. 4G), while the intensity of COL2 was decreased ($p < 0.001$; Fig. 4I). In the OAS group, the fluorescence intensity of MMP13 was decreased and that of COL2 was increased in comparison with the OA group (both $p < 0.05$). The images at a magnification (200 ×) were shown in Supplementary Fig. 4.

3.4. SMF promoted the number of CSPCs in the articular cartilage surface

Immunofluorescence double-staining such as CD166 and CD146, as well as CD105 and CD146, was performed to verify the effects of SMF on CSPCs in knee cartilage (Fig. 5A&C). The results showed that compared to the sham group, the $CD166^{+}CD146^{+}$ and $CD105^{+}CD146^{+}$ cells in the OA group were slightly increased (both $p < 0.001$; Fig. 5B&D). After SMF treatment for two weeks, the number of $CD166^{+}CD146^{+}$ and $CD105^{+}CD146^{+}$ cells in the articular cartilage surface was further increased (both $p < 0.001$). Immunohistochemical images of CD146 and CD166 in articular cartilage were shown in Supplementary Fig. 5.

3.5. SMF increased the expression of SDF-1 and CXCR4

To evaluate the change of SDF-1/CXCR4 signaling in response to SMF, SDF-1/CXCR4 signaling in the knee joint cartilage was assessed. Western blot analysis showed that the expression of CXCR4 was increased in knee cartilage after the induction of OA for two weeks ($p < 0.05$; Fig. 5E&F), while its expression in the OAS group was increased in comparison with the OA group ($p < 0.01$). Immunohistochemistry was consistent with this result (both $p < 0.001$; Fig. 5G&H). Immunofluorescence staining showed that compared to the sham group, $SDF\text{-}1^{+}$ cells in the OA knee cartilage were increased ($p < 0.001$; Fig. 5I&J) and further increased after SMF ($p < 0.001$).

3.6. SMF enhanced migration of BMSCs via SDF-1/CXCR4

To determine whether SMF would affect the migration ability of BMSCs, transwell and wound healing assays were conducted (Fig. 6A&C). Transwell invasion of BMSCs showed that compared to the sham group, the number of invaded cells was increased in the OA group ($p < 0.001$; Fig. 6B). However, the number of invaded cells was further increased in the OAS group ($p < 0.001$). Similarly, compared to the sham group, OA mouse-derived BMSCs promoted wound healing ($p < 0.001$; Fig. 6D), and SMF treatment further enhanced BMSCs' wound healing ability ($p < 0.01$).

To further examine the role of SDF-1/CXCR4 signaling in the migration of BMSCs, we used AMD3100, an inhibitor of CXCR4. The results showed that AMD3100 blocked SMF-driven migration and wound healing (both $p < 0.01$). There was no statistical difference between the OA and OAS groups regarding BMSCs' responses to the inhibitor.

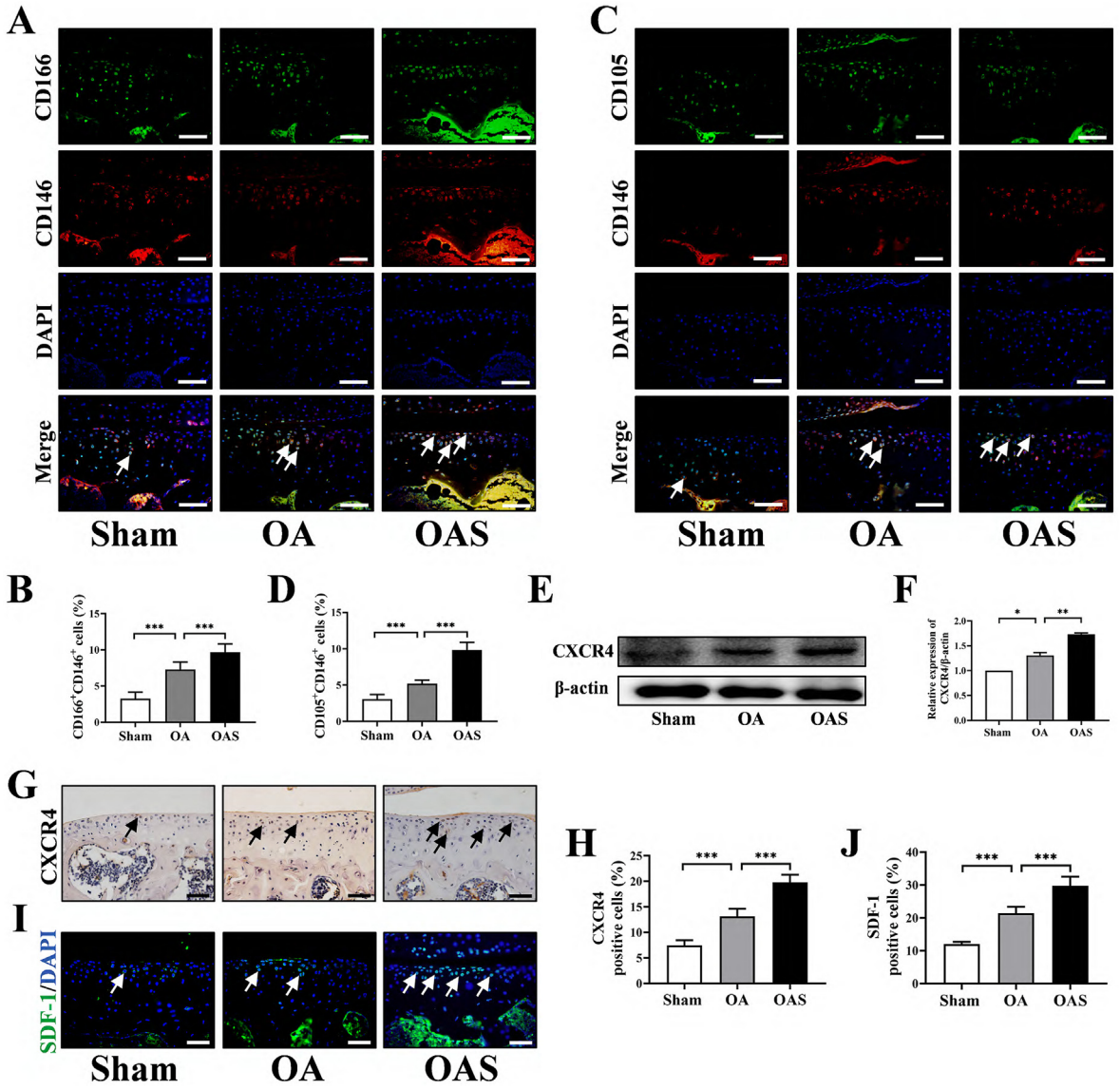

Figure 5. Effect of SMF on CSPCs in articular cartilage (A) Representative double immunofluorescent images of CSPCs-specific markers CD166 and CD146 in articular cartilage. Bar = 50 μm (B) Quantification of $CD166^{+}CD146^{+}$ cells in articular cartilage; n = 12 (C) Representative double immunofluorescence images of CD105 and CD146 in the coronal sections of articular cartilage. Bar = 50 μm (D) Quantification of $CD105^{+}CD146^{+}$ cells in articular cartilage; n = 12 (E–F) Western blot analysis, showing the protein level of CXCR4 and the relative quantification of the protein level of CXCR4 in articular cartilage; n = 3 (G) Representative immunohistochemical images of CXCR4 in articular cartilage. Bar = 50 μm (H) Quantification of $CXCR4^{+}$ cells in articular cartilage; n = 12 (I) Representative immunofluorescence images of SDF-1 in the coronal sections of articular cartilage. Bar = 50 μm (J) Quantification of $SDF\text{-}1^{+}$ cells in articular cartilage; n = 12. $^{**}p < 0.01$, $^{***}p < 0.001$.

3.7. SMF enhanced the expression of Piezo1 in mouse-derived BMSCs

To examine the effect of SMF on Piezo1, the level of Piezo1 in BMSCs was determined by immunofluorescence staining (Fig. 6E). Compared to the sham group, the intensity of red fluorescence, which indicated Piezo1, was increased ($p < 0.01$; Fig. 6F). The intensity of Piezo1 in the OAS group was further increased ($p < 0.05$). This result was verified with qRT-PCR and Western blot analysis (all $p < 0.05$; Fig. 6G–I).

3.8. SMF activated SDF-1/CXCR4 signaling pathway through Piezo1

We used ST2 mouse bone marrow stromal cell line and Piezo1 siRNA to explore the connection between Piezo1 and CXCR4 under SMF exposure *in vitro*. Immunofluorescence staining demonstrated that ST2 cells expressed Piezo1 (Fig. 7A), and its expression was validated by Western blot analysis (Fig. 7B). To probe the CXCR4-mediated mechanism of SMF's action, the CXCR4 level was determined by silencing Piezo1 in ST2 cells. The result of qRT-PCR and Western blot analysis showed that the interference efficiency of siRNA1 was higher than the other two Piezo1 siRNAs (siRNA2 and siRNA3) (all $p < 0.01$; Fig. 7C–E). Thus, Piezo1 siRNA1 was used for further experiments. ST2 cells, with or without Piezo1 siRNA1, were subjected to SMF. The mRNA and protein levels of CXCR4 were detected by qRT-PCR and Western blot analysis, respectively (Fig. 7F&H). SMF upregulated CXCR4 compared to the group without SMF and Piezo1 siRNA (both $p < 0.01$), and Piezo1 siRNA1 significantly decreased CXCR4 in ST2 cells (both $p < 0.01$). Importantly, SMF-induced CXCR4 was suppressed by silencing Piezo1 (both $p < 0.01$), and the result was consistent with immunofluorescence staining analysis (all $p < 0.05$; Fig. 7I&J).

4. Discussion

In this study, we described the role of SMF, a physiotherapeutic modality, in the relief of OA symptoms by examining the responses of

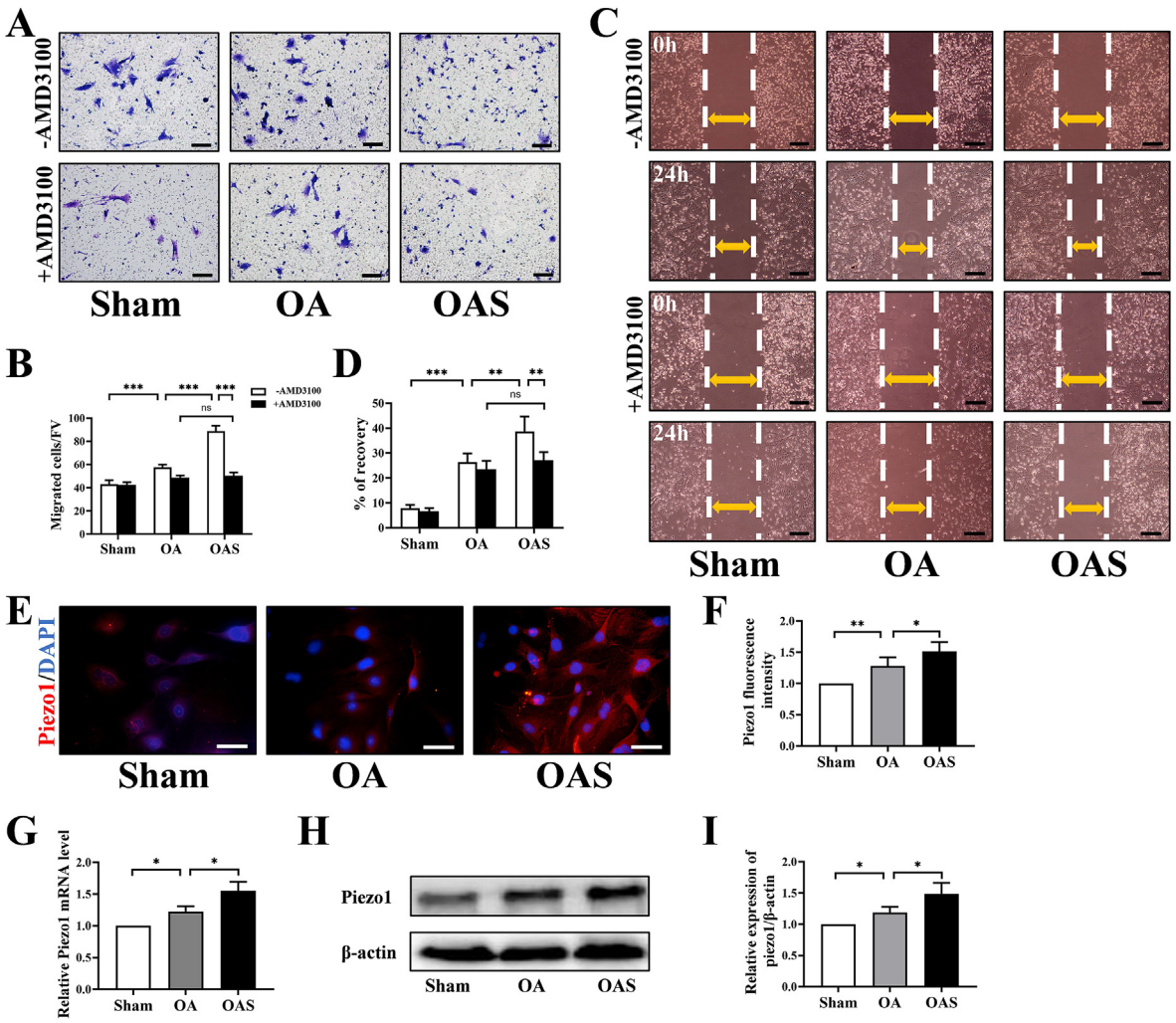

Figure 6. Induction of cell migration through regulating SDF-1/CXCR4 by SMF (A) Representative images of migration by crystal violet staining. BMSCs migration was stimulated by SMF, and the effect was blocked by the CXCR4 inhibitor, AMD3100. Bar = 200 μm (B) Quantitative analysis of BMSCs migratory; n = 3 (C) Representative images of BMSCs' wound healing. SMF stimulated BMSCs' wound healing, which was blocked by AMD3100. The white dotted line indicates the boundary of wound healing, and the yellow two-way arrow represents the width of the wound. Bar = 200 μm (D) Quantitative analysis of recovery; n = 3 (E) Representative immunofluorescence images of Piezo1 in mouse-derived BMSCs. Bar = 50 μm (F) Quantification of the fluorescence intensity of Piezo1 in mouse-derived BMSCs; n = 3 (G) The mRNA expression of Piezo1 in murine BMSCs was examined by qRT-PCR; n = 3 (H–I) Western blot analysis, showing the protein level of Piezo1 and the relative quantification of the protein level of Piezo1 in mouse-derived BMSCs; n = 3. $^{*}p < 0.05$, $^{**}p < 0.01$, $^{***}p < 0.001$, ns = not significant.

chondrogenesis and migration of endogenous stem cells. Our results showed that SMF improved the OARSI score in OA mice and decreased the ratio of calcified cartilage. The result also showed that SMF promoted the expression of SOX9 and COL2 in articular cartilage and decreased the expression of MMP13, thereby enhancing chondrogenesis and improving cartilage extracellular matrices. In addition, SMF not only promoted the number of CSPCs in the injured cartilage surface but also elevated CXCR4 via Piezo1, which enhanced the migration ability of BMSCs. These findings strongly indicated that SMF alleviated pathological cartilage degeneration (Fig. 8).

Compared to optical, acoustic, and electrical fields, magnetic fields have advantages because of their large force output, high precision, and deep tissue penetration [30]. While the effect of magnetic fields depends on parameters such as intensity, frequency and exposure time, there is no clear guideline on the magnetic parameters. Our previous studies showed that SMF-mediated induction of chondrogenesis and chondrocyte migration was intensity-dependent, with maximal responses observed at 200 mT SMF. Although >200 mT SMF was not tested here, it is reported that 500 mT SMF may affect neurogenesis in mice, suggesting that higher SMF intensity may have deleterious effects [31].

Articular cartilage bears gravitational loads and lubricates joints. Chondrocytes produce and maintain extracellular matrices, which are rich in COL2 and proteoglycan [32]. Due to the lack of blood vessels, nerves, and lymphatic vessels, a spontaneous repair of cartilage defects, caused by OA, aging, or joint damage, is not possible [33]. Biophysical forces such as electromagnetic fields and SMFs, are of interest because of their role in bone remodeling and wound healing [34]. For example, it is reported that a moderate-intensity (40 mT) SMF resulted in histological improvement of rabbit cartilage extracellular matrix [35], and SMF (600 mT) exposure for 72 h stimulated the growth of human chondrocytes *in vitro* [34]. SMF (140 mT) regulated T-type calcium channels and mediated MSC proliferation through the MAPK signaling pathway [11], while SMF (280 mT) improved chondrogenesis and proliferation of mandibular bone marrow mesenchymal stem cells (MBMSCs) in the MBMSC/mandibular condylar chondrocyte coculture system [8]. The present study revealed that SMF reduced articular cartilage destruction. For the restoration of joint function, both chondrocytes and extracellular matrices are involved. This study revealed that SMF promoted chondrogenesis of BMSCs by elevating SOX9 and improved the cartilage extracellular matrices by increasing COL2 and decreasing MMP13.

It is recently reported that CSPCs in articular cartilage co-express CD166, CD146, and CD105. When articular cartilage is damaged, these

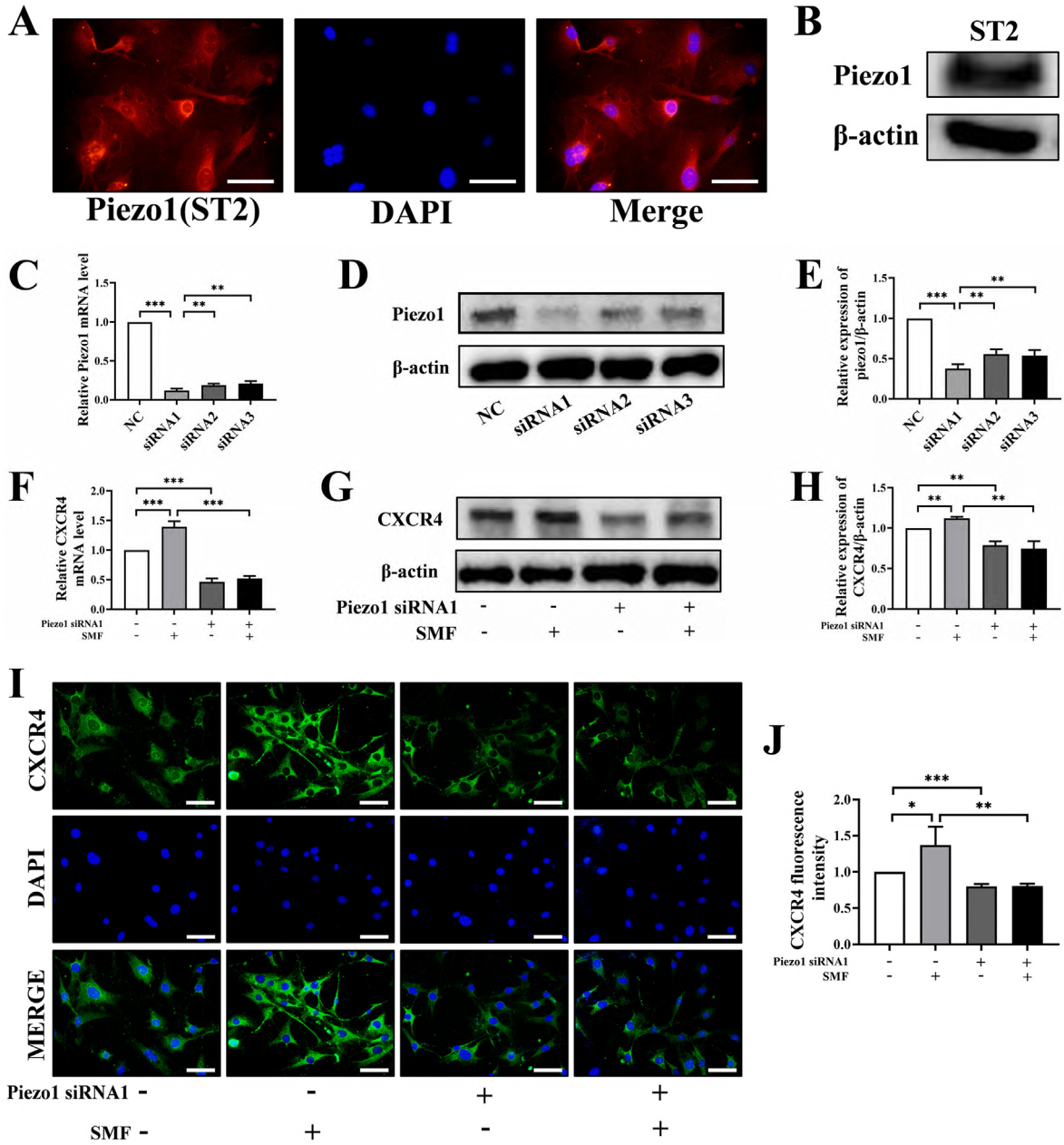

Figure 7. Regulation of the CXCR4 through Piezo1 by SMF *in vitro* (A) Piezo1 expression (red staining), counterstained with DAPI (blue staining), was examined in ST2 cells. Bar = 50 μm (B) Piezo1 expression was examined by Western blot analysis in ST2 cells (C) The mRNA expression levels of Piezo1 with Piezo1 siRNA1, 2, and 3 were examined by qRT-PCR in ST2 cells (D) Western blot analysis, showing the protein level of Piezo1 with Piezo1 siRNA1, 2, and 3 in ST2 cells (E) The relative quantification of the protein level of Piezo1 (F) The mRNA expression levels of CXCR4 with or without SMF and Piezo1 siRNA1 were examined by qRT-PCR in ST2 cells (G–H) Western blot analysis, showing the protein level of CXCR4 and the relative quantification of the protein level of CXCR4 in ST2 cells with or without SMF and Piezo1 siRNA1 (I–J) Representative immunofluorescence images of CXCR4 and the quantification of the fluorescence intensity of CXCR4 in ST2 cells with or without SMF and Piezo1 siRNA1. Bar = 50 μm. Each group was expressed as the mean ± SD of three independent experiments. $^{*}p < 0.05$, $^{**}p < 0.01$, $^{***}p < 0.001$.

cells proliferate, migrate, and adhere to the site of injury [16]. However, their ability to repair cartilage is limited. In the study, the effect of SMF on CSPCs was evaluated by immunohistochemistry and immunofluorescence staining. The results showed that two weeks after SMF exposure, the presence of CSPCs on the articular cartilage surface was increased. Because of the technical issues, we could not extract a sufficient amount of CSPCs, and thus we used BMSCs and ST2 cells to observe and explore the therapeutic effect and mechanism of SMF.

A homing rate of MSCs to target organs is reported limited and this limitation could seriously affect the repair efficacy of target organs. Effective therapy requires MSCs to reach the site of injury [20]. SDF-1 is considered the main regulator of $CXCR4^{+}$ MSCs. It plays an important role in the migration of $CXCR4^{+}$ MSCs to injury sites and regulates repair activities [36]. Increasing SDF-1 or CXCR4 can improve the homing efficiency of MSCs [21]. It is reported that ultrasound combined with SDF-1 promoted the homing of BMSCs to cartilage [20], and low-intensity pulsed ultrasound increased SDF-1 and CXCR4 and promoted MSCs migration [21]. SMF has been found to enhance the migration of dental pulp stem cells [10]. In this study, SMF increased SDF-1 and CXCR4 in the mouse model of OA. The inhibitor of the CXCR4, AMD3100, was used to study whether SMF regulated the migration of BMSCs by regulating SDF-1/CXCR4. The results showed that the effect of SMF on SDF-1/CXCR4 signaling was significantly inhibited by AMD3100.

Piezo1 is a molecular sensor for cells to sense and respond to

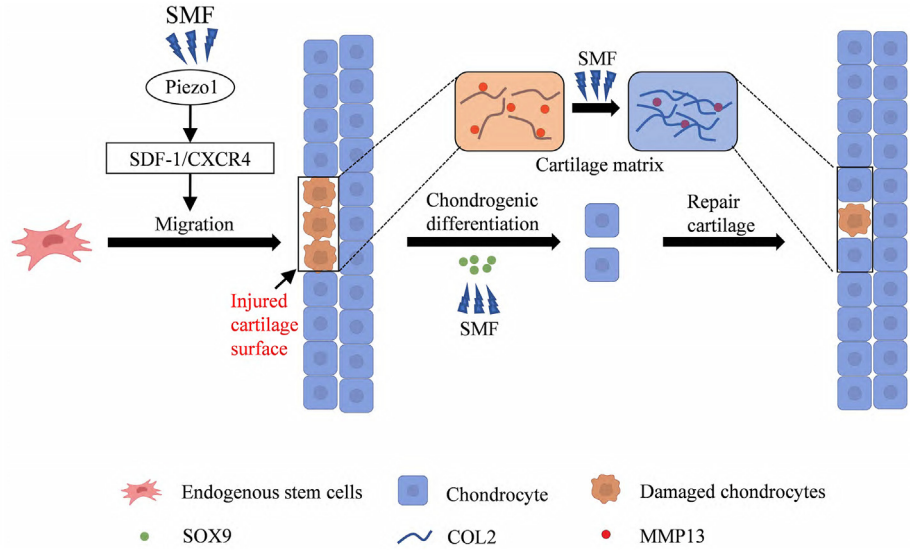

Figure 8. The proposed SMF-driven migration of endogenous stem cells, chondrogenesis, and cartilage matrix improve articular cartilage in a mouse model of OA.

mechanical forces. Piezo1 is embedded in the cell membrane, and it converts extracellular mechanical stimuli into intracellular biochemical signals [37]. MSCs are mechanosensitive [38], and SMF provides biophysical stimuli [39]. In our study, SMF increased Piezo1 in the BMSCs and transformed mechanical signals into biological signals *in vivo*. Mousawi et al. have shown that chemical activation of Piezo1 channels can drive the migration of MSCs [38]. SDF-1/CXCR4 is a primary regulatory axis to promote stem cell homing [40]. Our results showed that compared to the control group, CXCR4 in the Piezo1 siRNA1-treated group was significantly reduced. SMF exposure significantly increased CXCR4 in ST2 cells, and Piezo1 siRNA1 reduced SMF-driven CXCR4 expression. Collectively, the results demonstrated that SMF promoted the expression of CXCR4 by activating Piezo1.

This study has limitations. The progression of OA symptoms was not easily predicted. Since the phenotypic alterations were not detected 2 weeks after surgery, follow-up experiment is needed to evaluate the outcome after 4 and 8 weeks. The isolation of CSPCs was not reproducibly conducted because of technical difficulties. It is thus recommended to further evaluate the contribution of CSPCs in the role of SMF and the progression of OA.

5. Conclusion

In conclusion, this study demonstrates that SMF provides a novel physical therapy option for OA by regulating not only chondrogenesis but also the migration of endogenous stem cells. The migration-promoting effects of SMF are mediated by Piezo1 and SDF-1/CXCR4 signaling, which may serve as a therapeutic target for OA.

Author contributions

PZ and YS designed research; YS, YF, XL, and JL conducted research; YS, DL, LZ, and YM collected the data; PZ, YS, MW, and ZL analyzed the data; PZ and YS wrote the manuscript; PZ, YS, LY, YY, and HY revised the manuscript; PZ approved the final manuscript as submitted; PZ accepted responsibility for the integrity of data analysis.

Funding

This work was supported by grants from the National Natural Science Foundation of China (81772405 and 81572100 to PZ), and the Heye Health Technology Chongming Project (HYCMP-2021006 to PZ).

Declaration of competing interest

The authors declare that they have no competing financial interests.

Acknowledgements

All persons who have made substantial contributions to the work reported in the manuscript (e.g., technical help, writing and editing assistance, general support), but who do not meet the criteria for authorship, are named in the Acknowledgements and have given us their written permission to be named. If we have not included an Acknowledgements, then that indicates that we have not received substantial contributions from non-authors.

Appendix A. Supplementary data

Supplementary data to this article can be found online at https://doi.org/10.1016/j.jot.2022.11.007.

References

[1] Glyn-Jones S, Palmer AJ, Agricola R, Price AJ, Vincent TL, Weinans H, et al. Osteoarthritis. Lancet. 2015;386(9991):376–87.
[2] Meurot C, Jacques C, Martin C, Sudre L, Breton J, Rattenbach R, et al. Targeting the GLP-1/GLP-1R axis to treat osteoarthritis: a new opportunity? J Orthop Translat 2022;32:121–9.
[3] Zhu J, Yang S, Qi Y, Gong Z, Zhang H, Liang K, et al. Stem cell-homing hydrogel-based miR-29b-5p delivery promotes cartilage regeneration by suppressing senescence in an osteoarthritis rat model. Sci Adv 2022;8(13):eabk0011.
[4] Zheng W, Li X, Li J, Wang X, Liu D, Zhai L, et al. Mechanical loading mitigates osteoarthritis symptoms by regulating the inflammatory microenvironment in a mouse model. Ann N Y Acad Sci 2022;1512(1):141–53.
[5] Zhang Y, Li X, Li J, Liu D, Zhai L, Wang X, et al. Knee loading enhances the migration of adipose-derived stem cells to the osteoarthritic sites through the SDF-1/CXCR4 regulatory axis. Calcif Tissue Int 2022;111(2):171–84.
[6] Zhang G, Zhen C, Yang J, Zhang Z, Wu Y, Che J, et al. 1-2 T static magnetic field combined with Ferumoxytol prevent unloading-induced bone loss by regulating iron metabolism in osteoclastogenesis. J Orthop Translat 2022;38:126–40.
[7] Yang J, Zhou S, Lv H, Wei M, Fang Y, Shang P. Static magnetic field of 0.2-0.4 T promotes the recovery of hindlimb unloading-induced bone loss in mice. Int J Radiat Biol 2021;97(5):746–54.
[8] Zhang M, Li W, He W, Xu Y. Static magnetic fields enhance the chondrogenesis of mandibular bone marrow mesenchymal stem cells in coculture systems. BioMed Res Int 2021;2021:9962861.
[9] Zhang J, Meng X, Ding C, Shang P. Effects of static magnetic fields on bone microstructure and mechanical properties in mice. Electromagn Biol Med 2018;37(2):76–83.
[10] Zheng L, Zhang L, Chen L, Jiang J, Zhou X, Wang M, et al. Static magnetic field regulates proliferation, migration, differentiation, and YAP/TAZ activation of human dental pulp stem cells. J Tissue Eng Regen Med 2018;12(10):2029–40.

[11] Wu H, Li C, Masood M, Zhang Z, González-Almela E, Castells-Garcia A, et al. Static magnetic fields regulate T-type calcium ion channels and mediate mesenchymal stem cells proliferation. Cells 2022;11(15):2460.
[12] Nguyen TH, Duong CM, Nguyen XH, Than UTT. Mesenchymal stem cell-derived extracellular vesicles for osteoarthritis treatment: extracellular matrix protection, chondrocyte and osteocyte physiology, pain and inflammation management. Cells 2021;10(11):2887.
[13] Parate D, Kadir ND, Celik C, Lee EH, Hui JHP, Franco-Obregón A, et al. Pulsed electromagnetic fields potentiate the paracrine function of mesenchymal stem cells for cartilage regeneration. Stem Cell Res Ther 2020;11(1):46.
[14] Song H, Park KH. Regulation and function of SOX9 during cartilage development and regeneration. Semin Cancer Biol 2020;67(Pt 1):12–23.
[15] Kanazawa T, Furumatsu T, Hachioji M, Oohashi T, Ninomiya Y, Ozaki T. Mechanical stretch enhances COL2A1 expression on chromatin by inducing SOX9 nuclear translocalization in inner meniscus cells. J Orthop Res 2012;30(3):468–74.
[16] Jiang Y, Tuan RS. Origin and function of cartilage stem/progenitor cells in osteoarthritis. Nat Rev Rheumatol 2015;11(4):206–12.
[17] Riegger J, Palm HG, Brenner RE. The functional role of chondrogenic stem/progenitor cells: novel evidence for immunomodulatory properties and regenerative potential after cartilage injury. Eur Cell Mater 2018;36:110–27.
[18] Zheng J, Lin Y, Tang F, Guo H, Yan L, Hu S, et al. Promotive role of circATRNL1 on chondrogenic differentiation of BMSCs mediated by miR-338-3p. Arch Med Res 2021;52(5):514–22.
[19] Fu X, Liu G, Halim A, Ju Y, Luo Q, Song AG. Mesenchymal stem cell migration and tissue repair. Cells 2019;8(8):784.
[20] Xiang X, Liu H, Wang L, Zhu B, Ma L, Du F, et al. Ultrasound combined with SDF-1α chemotactic microbubbles promotes stem cell homing in an osteoarthritis model. J Cell Mol Med 2020;24(18):10816–29.
[21] Xia P, Wang X, Wang Q, Wang X, Lin Q, Cheng K, et al. Low-intensity pulsed ultrasound promotes autophagy-mediated migration of mesenchymal stem cells and cartilage repair. Cell Transplant 2021;30:963689720986142.
[22] Zhu J, Liu Y, Chen C, Chen H, Huang J, Luo Y, et al. Cyasterone accelerates fracture healing by promoting MSCs migration and osteogenesis. J Orthop Translat 2021;28:28–38.
[23] Xu X, Liu S, Liu H, Ru K, Jia Y, Wu Z, et al. Piezo channels: awesome mechanosensitive structures in cellular mechanotransduction and their role in bone. Int J Mol Sci 2021;22(12):6429.
[24] Zheng W, Ding B, Li X, Liu D, Yokota H, Zhang P. Knee loading repairs osteoporotic osteoarthritis by relieving abnormal remodeling of subchondral bone via Wnt/β-catenin signaling. Faseb J 2020;34(2):3399–412.
[25] Zheng W, Li X, Liu D, Li J, Yang S, Gao Z, et al. Mechanical loading mitigates osteoarthritis symptoms by regulating endoplasmic reticulum stress and autophagy. Faseb J 2019;33(3):4077–88.
[26] Li X, Yang J, Liu D, Li J, Niu K, Feng S, et al. Knee loading inhibits osteoclast lineage in a mouse model of osteoarthritis. Sci Rep 2016;6:24668.
[27] Song J, Liu L, Lv L, Hu S, Tariq A, Wang W, et al. Fluid shear stress induces Runx-2 expression via upregulation of PIEZO1 in MC3T3-E1 cells. Cell Biol Int 2020;44(7):1491–502.
[28] Wang X, Li X, Li J, Zhai L, Liu D, Abdurahman A, et al. Mechanical loading stimulates bone angiogenesis through enhancing type H vessel formation and downregulating exosomal miR-214-3p from bone marrow-derived mesenchymal stem cells. Faseb J 2021;35(1):e21150.
[29] Abdurahman A, Li X, Li J, Liu D, Zhai L, Wang X, et al. Loading-driven PI3K/Akt signaling and erythropoiesis enhanced angiogenesis and osteogenesis in a postmenopausal osteoporosis mouse model. Bone 2022;157:116346.
[30] Wang X, Law J, Luo M, Gong Z, Yu J, Tang W, et al. Magnetic measurement and stimulation of cellular and intracellular structures. ACS Nano 2020;14(4):3805–21.
[31] Ho SY, Chen IC, Chen YJ, Lee CH, Fu CM, Liu FC, et al. Static magnetic field induced neural stem/progenitor cell early differentiation and promotes maturation. Stem Cell Int 2019;2019:8790176.
[32] Ye C, Chen J, Qu Y, Qi H, Wang Q, Yang Z, et al. Naringin in the repair of knee cartilage injury via the TGF-β/ALK5/Smad2/3 signal transduction pathway combined with an acellular dermal matrix. J Orthop Translat 2021;32:1–11.
[33] Li L, Yu F, Zheng L, Wang R, Yan W, Wang Z, et al. Natural hydrogels for cartilage regeneration: modification, preparation and application. J Orthop Translat 2018;17:26–41.
[34] Amin HD, Brady MA, St-Pierre JP, Stevens MM, Overby DR, Ethier CR. Stimulation of chondrogenic differentiation of adult human bone marrow-derived stromal cells by a moderate-strength static magnetic field. Tissue Eng 2014;20(11–12):1612–20.
[35] Jaberi FM, Keshtgar S, Tavakkoli A, Pishva E, Geramizadeh B, Tanideh N, et al. A moderate-intensity static magnetic field enhances repair of cartilage damage in rabbits. Arch Med Res 2011;42(4):268–73.
[36] Wang X, Wang C, Gou W, Xu X, Wang Y, Wang A, et al. The optimal time to inject bone mesenchymal stem cells for fracture healing in a murine model. Stem Cell Res Ther 2018;9(1):272.
[37] Hao L, Li L, Wang P, Wang Z, Shi X, Guo M, et al. Synergistic osteogenesis promoted by magnetically actuated nano-mechanical stimuli. Nanoscale 2019;11(48):23423–37.
[38] Mousawi F, Peng H, Li J, Ponnambalam S, Roger S, Zhao H, et al. Chemical activation of the Piezo1 channel drives mesenchymal stem cell migration via inducing ATP release and activation of P2 receptor purinergic signaling. Stem Cell 2020;38(3):410–21.
[39] Huyan T, Peng H, Cai S, Li Q, Dong D, Yang Z, et al. Transcriptome analysis reveals the negative effect of 16 T high static magnetic field on osteoclastogenesis of RAW264.7 cells. BioMed Res Int 2020;2020:5762932.
[40] Zhou C, Xu AT, Wang DD, Lin GF, Liu T, He FM. The effects of Sr-incorporated micro/nano rough titanium surface on rBMSC migration and osteogenic differentiation for rapid osteointegration. Biomater Sci 2018;6(7):1946–61.

Ping Zhang